ACS Sustainable Chemistry & Engineering

pubs.acs.org/journal/ascecg

Research Article

Adhesive and Antibacterial Films Based on Marine-Derived Fucoidan and Chitosan

Cátia Correia, Diana Soares da Costa, Ana Rita Inácio, A. Catarina Vale, Daniela Peixoto, Tiago H. Silva, Rui L. Reis, Iva Pashkuleva, and Natália M. Alves*

Cite This: https://doi.org/10.1021/acssuschemeng.2c05144

Read Online

ACCESS | Metrics & More | Article Recommendations | Supporting Information

ABSTRACT: Marine-derived polymers are environmentally friendly and sustainable biomaterials that have structural similarities with the main components of the extracellular matrix. Moreover, some marine polymers have specific bioactivity that can be transferred to the systems made of these biomolecules. Herein, we developed antibacterial adhesive films combining two marine polysaccharides, namely, fucoidan and chitosan. Fucoidan was functionalized with catechol groups (FCat) to improve its adhesive properties. This modification enhanced also the fucoidan antibacterial properties: while fucoidan is active against Gram-positive bacteria, FCat showed bactericidal activity against Gram-positive and Gram-negative bacteria. To improve the processability and mechanical properties, FCat was blended with chitosan and solvent-casted to obtain films. These films exhibited an adhesion strength similar to the one of clinically used natural adhesives and no cytotoxicity: fibroblastic cells attached and remained viable on the films. Altogether our results demonstrated that the developed antibacterial and adhesive films are a feasible alternative of cytotoxic synthetic adhesives used for soft tissue healing applications.

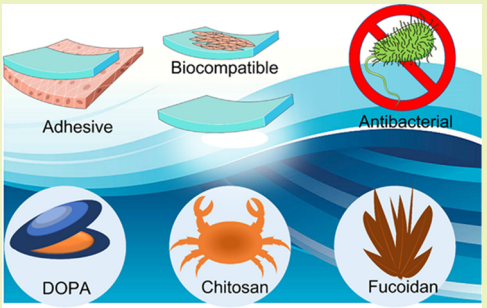

KEYWORDS: *sustainable biomaterials, biomimetic adhesives, antibacterial films, marine polysaccharides*

1. INTRODUCTION

The development of biomaterials for soft tissue engineering and wound healing remains challenging because of the requirements for antibacterial properties and adhesion between the material and tissue to promote the treatment efficacy.[1] Nowadays, infections continue to be the most severe risk associated with implant failure,[2] and thus, antibacterial biomaterials that promote tissue healing are demanded.[3] Marine ecosystems rich in microalgae and macroalgae, such as seaweeds, are known to combat different bacteria.[4] Such ecosystems contain different components, but among them, fucoidan, an anionic sulfated polysaccharide that is fucose-rich, has been identified in the cell wall matrix of brown seaweeds and described for its antibacterial properties.[5,6] Fucoidan is neither toxic nor irritating[6] and has been proposed for anticoagulant,[7] antioxidant,[8] angiogenic,[9,10] antitumoral,[11,12] antiviral,[13−15] anti-inflammatory,[16,17] and antibacterial[18] applications. However, its bioactivity depends on the molecular weight, the extraction and purification procedures, and structure (e.g., branching, sugar and sulfate content, and sulfate group positions).[19] In tissue engineering (TE), fucoidan has been used to promote fibroblast proliferation[20] and enhance the activity of fibroblast growth factor-2 (FGF-2).[21] Herein, we propose to extend these applications of fucoidan to soft TE and wound healing applications. To this end, fucoidan should be rendered adhesive to promote its tight attachment to the tissue and enhance healing.[22] The marine adhesive proteins (MAPs) secreted by mussels are well-known bio-adhesives that are efficient in wet environments because of the content of 3,4-dihydroxyphenyl-L-alanine (L-DOPA)/catechol groups.[23−25] Recently, we have demonstrated that fucoidan can be modified with dopamine and the obtained derivative is significantly more adhesive than the nonmodified fucoidan.[26] Herein, we assessed the antibacterial activity of fucoidan obtained from two different brown *algae* species (*Fucus vesiculosus* and *Bifurcaria bifurcata*) and catechol-conjugated fucoidan.

Applications in TE and wound healing also require feasible processing into devices with appropriate mechanical properties. We propose blending as a strategy to achieve this requirement. Because the use of polymers from marine sources avoids the risk of infections and immunogenicity and has no limitations related to religious or ethical issues, as a second component of the blend, we have selected another marine-derived polymer, namely, chitosan, a cationic polysaccharide obtained from the chitin of the crustacean shells through a deacetylation process.[27] Chitosan is biodegradable and biocompatible,[28] and together with fucoidan, it can be processed into nanoparticles,[29]

Received: August 28, 2022
Revised: November 17, 2022

hydrogels,[30] polyelectrolyte multilayers,[21] or sponges.[31] In this work, chitosan was blended with fucoidan or catechol-conjugated fucoidan. The blends were processed in the form of films, an adequate geometry for their potential application as wound dressings, and their bioadhesive, biocompatible, and antibacterial properties were evaluated.

2. EXPERIMENTAL SECTION

2.1. Materials. Medium molecular weight chitosan (~310 kDa, determined by gel permeation chromatography, GPC) was obtained from Sigma-Aldrich. Chitosan was deacetylated (degree of deacetylation: ~99%, determined by ^{1}H-NMR) and purified by a series of filtration and precipitation steps in water and ethanol, followed by freeze drying according to the protocol described by Signini and Campana.[32] Fucoidan from *Fucus vesiculosus* (*F. vesiculosus*) was purchased from Sigma-Aldrich (batch number: SLBW1602, molecular weight of 103 kDa measured by GPC with multiangle laser light scattering (MALLS) detector and a sulfation degree of 9% were provided by the supplier). Mouse fibroblast cell line L929 was obtained from Sigma-Aldrich partnered with the European Collection of authenticated cell cultures (ECACC, UK). Dulbecco's modified minimum essential medium (DMEM), sodium bicarbonate ($NaHCO_3$), phalloidin−tetramethylrhodamine B isothiocyanate fluorescent dye, bovine serum albumin (BSA), dopamine hydrochloride, N-(3-dimethylaminopropyl)-N′-ethylcarbodiimide hydrochloride (EDC), 2-(N-morpholino)ethanesulfonic acid buffer (MES), Mueller Hinton Broth (MHB), and Mueller Hinton agar (MHA) were also purchased from Sigma-Aldrich. Dialysis membrane spectra/Por 3 (cutoff 3.5 kDa, width 54 mm, diameter 34 mm) were purchased from Fisher Scientific. Alamar blue was obtained from Bio-Rad. Antibiotic/antimycotic, Dulbecco's phosphate buffered saline (DPBS), trypLE express (1×) with phenol red, fetal bovine serum (FBS), Calcein AM, and propidium iodide (PI) were ordered from Thermo-Fisher Scientific. 4′,6-Diamidino-2-phenylindole (DAPI) was obtained from Biotium Inc., Alcian Blue 8GX was purchased from DiaPath, and glycerol and acetic acid were ordered from Honeywell (North Caroline, USA). Sodium chloride (NaCl) and sodium hydroxide (NaOH) were purchased from PanReac AppliChem.

2.2. Extraction of Fucoidan. Fucoidan was extracted from *Bifurcaria bifurcata* (*B. bifurcata*) based on the methodology described by Yang et al.[33] The *algae* were collected at the Aver-o-Mar beach (Portugal) and then pretreated with 85% ethanol for approximately 12 h, followed by an acetone wash and drying. Extraction was carried out with distilled water at 65 ± 5 °C for 1 h. The obtained extract was centrifuged at 20,000 *g* for 15 min and the supernatant was treated with 1% (v/v) $CaCl_2$ and kept overnight at 4 °C. The fraction was removed by centrifugation (20,000 *g*) and left at 4 °C for 4 h to promote the precipitation of some impurities. After centrifugation, absolute ethanol was added to the supernatant and left at 4 °C overnight. The precipitated polysaccharide was recovered by centrifugation, washed with ethanol and acetone, and vacuum-dried at room temperature (RT). Then, the fucoidan was characterized by Fourier transform infrared (FTIR) and ^{1}H-NMR spectroscopies and compared with commercial fucoidan from *F. vesiculosus*.

2.3. Modifications of Fucoidan. Fucoidan was modified according to the procedure proposed by Jeong et al.[26] Briefly, fucoidan (1 g) was dissolved in 150 mL of MES buffer (0.1 M, pH = 6, 1 h). EDC (2.05 g) and dopamine (1.24 g) were added to the solution and the reaction mixture was stirred for 2 h at RT. The solution was dialyzed against distilled water (cutoff 3.5 kDa, 24 h) to remove unreacted coupling reagents. The final product was freeze-dried and kept at 4 °C until use.

2.4. Assessment of Fucoidan Antibacterial Properties. Two different strains, namely, Gram-negative *Escherichia coli* (*E. coli*) (ATCC 25922) and Gram-positive *Staphylococcus aureus* (*S. aureus*) (ATCC 25923), were used to determine the minimum bactericidal concentration (MBC) of different fucoidans (commercial and extracted by us) and catechol-conjugated commercial fucoidan (FCat). *E. coli* and *S. aureus* strains were cultured on MHB (37 °C, 60 rpm) and the microbial suspension was adjusted to 1.0×10^6 CFU/mL. Fucoidan obtained from different sources and FCat were dissolved in sterile water (200 mg/mL). These stock solution were diluted to prepare a series of solutions with different concentrations (1, 2, 5, 10, 25, 50, and 100 mg/mL) that were tested using the following procedure. In a 96-well plate, 50 μL of bacterial suspension was added to 50 μL of the fucoidan solution. The plate was incubated at 37 °C for 24 h. Then, aliquots from each well (10 μL) were added on the surface of nutrient MHA and incubated at 37 °C for 24 h. MBC was determined as the lowest concentration that shows no bacterial growth on the agar plate. Several controls were used: bacterial suspension without fucoidan, bacterial suspension with ampicillin (50 mg/mL), and different concentrations of fucoidan without a bacterial suspension. All assays were performed in triplicate.

2.5. Film Casting. The films were obtained from chitosan solution (1.5% w/v in 0.15 M NaCl) with aq. acetic acid (1.5% v/v) and glycerol (5% v/v) to which 0.5% w/v of fucoidan or modified fucoidan was added (Table S1 in the Supporting Information). The solution was solvent-casted in a Petri dish (Ø = 90 mm) or directly in a 24 well plate for the biological assays and dried at 37 °C for 48 h. The dried films were neutralized using 1 M NaOH for 5 min, followed by washing with distilled water until neutral pH. The obtained films are designated as Chit (single-component films from chitosan used as a control), Chit/F (blended films obtained from chitosan and unmodified fucoidan), and Chit/FCat (blended films obtained from chitosan and modified fucoidan).

2.6. Surface Characterization of the Films. Surface chemistry of the films was analyzed by X-ray photoelectron spectroscopy (XPS, spectroscope Axis supra, Kratos) equipped with monochromatic AI-Kα radiation at 1486.6 eV. Photoelectrons were collected from a take-off angle of 90° relative to the film surface. Each measurement was done in a Constant Analyzer Energy (CAE) mode with a pass energy of 160 eV for survey spectra and 40 eV for high-resolution spectra. The C1s binding peak at 285 eV corresponding to a hydrocarbon peak was used as a reference.[34] Data analysis and atomic concentration were determined from the XPS peaks of high-resolution scans using ESCape software (Kratos).

Alcian blue staining was performed to visualize the distribution of the fucoidan on the surface of the films. The films were gently shaken in a solution of Alcian blue (1% Alcian blue dissolved in 3% of acetic acid, pH = 2.5) for 1 h, followed by several washes with PBS, until the blue background had been removed. The films were observed under a microscope Leica DM750.

Surface hydrophilicity and surface energy of the films were obtained using two testing liquids, namely, water and diiodomethane, and Owens, Wendt, Rabel, and Kaeble (OWRK) equation. The contact angles were measured with goniometer OCA 15+ (DataPhysics, Germany) equipped with a motor syringe for droplet deposition. The testing liquid (3 μL for water and 1 μL for diiodomethane) was placed on the film and an image was recorded and analyzed by SCA20 software (DataPhysics, Germany). The surface energy and the respective polar and dispersive components were determined using the following input parameters from the SCA20 software database: water surface energy of 72 mN m^{-1} (dispersive component (γ_d) = 19.90 mN m^{-1} and polar component (γ_p) 52.20 mN m^{-1}) and diiodomethane surface energy of 50 mN m^{-1} (γ_d = 47.40 mN m^{-1} and γ_p = 2.60 mN m^{-1}).

2.7. Mechanical Properties. Tensile strength tests were performed with Universal Mechanical Testing Equipment (INSTRON 5540), equipped with a load cell of 50 N, under tensile mode. The films were cut into strips (5×25 mm^2) and soaked in PBS solution at RT. The thickness of each sample was measured using a digital micrometer (Mitutoyo, Japan). The samples were positioned between the two grips of the equipment at a distance of 1 cm in the length axis, and the measurements were carried out under a cross-head speed of 1 mm/min until film rupture. Five specimens were tested per condition and based on the experimental stress−strain curve, the main mechanical parameters tensile strength, elongation at break, and Young's modulus were calculated for each film.

2.8. Adhesion Properties. The adhesion strength of the films was assessed using a Universal Mechanical Testing Equipment (Instron

https://doi.org/10.1021/acssuschemeng.2c05144
ACS Sustainable Chem. Eng. XXXX, XXX, XXX−XXX

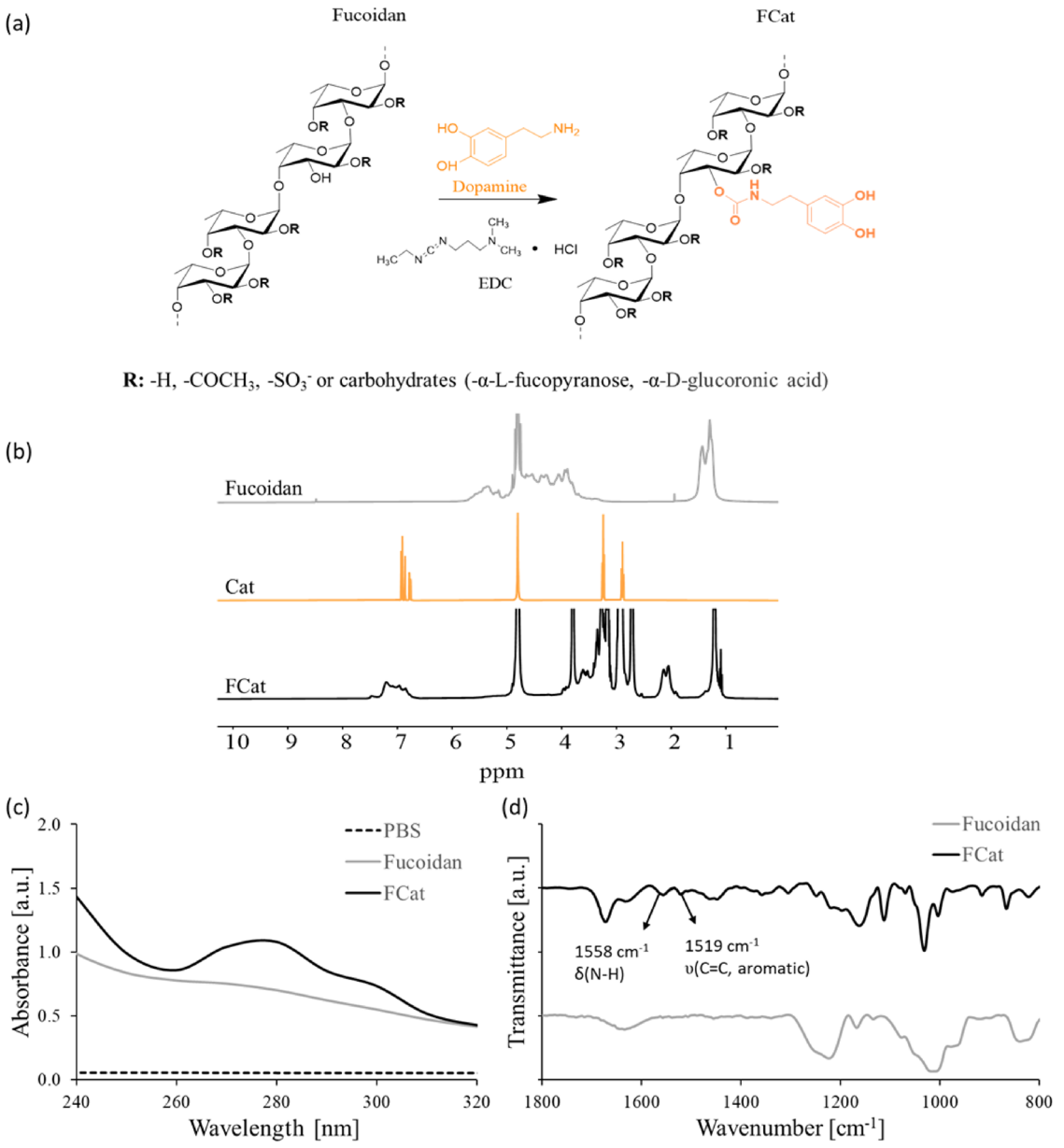

Figure 1. Modification and characterization of fucoidan: (a) Schematic presentation of the reaction used to modify fucoidan (FCat); (b) Nuclear magnetic resonance (^{1}H-NMR) spectra of fucoidan (gray), dopamine (orange), and FCat (black); (c) UV−vis spectra of fucoidan (2 mg/mL, gray) and FCat (2 mg/mL, black); (d) FTIR spectra of fucoidan and FCat.

5540) with a load cell of 50 N, following an adjustment of the lap-shear test described in the ASTM D1002 standard procedure. Briefly, the films were cut in stripes (10 × 30 mm^2) and two strips were vertically overlaid to achieve an overlapping area of 10 × 10 mm^2. The overlapped strips were placed between two glass slides, clamped tightly, and immersed in PBS solution at 37 °C. Then, the glasses were removed, and each extremity of the bonded strips was positioned between the grips of the mechanical testing machine at 20 mm of distance, and an axial tensile force was applied at a constant cross-head speed (3 mm/min). The resulting stress−strain curve was used to determine the adhesion strength of the films by the following equation:

$$\text{lap} - \text{shear adhesion (Pa)} = \frac{\text{Force (N)}}{\text{area of adhesive overlap (m}^2\text{)}} \quad (1)$$

2.9. Cellular Assays. L929 mouse fibroblast cells (NCTC clone 929, ATCC CCL-1, passage P30 and 31) were used to test the in vitro cytotoxicity of films. Cells were cultured in DMEM with low glucose and phenol red, supplemented with 10% FBS and 1% antibiotic−antimycotic solution. Cells were incubated at 37 °C in a humidified air atmosphere of 5% CO_2. The medium was changed every 3 days. At 90% of confluence, cells were washed with DPBS and detached with 5 mL of trypLE express solution for 5 min at 37 °C. To inactivate the trypLE, 10 mL of the culture medium was added. The cells were centrifuged at 300 rcf for 5 min, and the obtained pellet was resuspended in the culture medium. Films (Ø = 13 mm) were sterilized by UV (30 min each side) followed by immersion in 70% (v/v) ethanol (30 min). The sterile films were washed with DPBS, immersed in DMEM without FBS (24 h), placed in a 24-wells plate, and 200 μL of a cell suspension in DMEM culture medium (3 × 10^5 cells/mL) was added to each well. Tissue culture polystyrene (TCPS) was used as a control. Samples were incubated at 37 °C in a humidified air atmosphere of 5% CO_2. After 3 h of seeding, a fresh culture medium was added to each well until 1 mL of volume.

The metabolic activity of L929 fibroblastic cells was determined by the Alamar blue assay after 1, 3, 7, 14, and 21 days of culture. At these time points, the culture medium was replaced with a fresh medium

https://doi.org/10.1021/acssuschemeng.2c05144
ACS Sustainable Chem. Eng. XXXX, XXX, XXX−XXX

Table 1. Antibacterial Activity of Fucoidan from Different Sources and Modified Fucoidan (FCat) against *E. coli* and *S. aureus*[a]

concentration (mg/mL)	fucoidan (*B. bifurcata*)*E. coli*	fucoidan (*B. bifurcata*)*S. aureus*	fucoidan (*F. vesiculosus*)*E. coli*	fucoidan (*F. vesiculosus*)*S. aureus*	FCat fucoidan (*F. vesiculosus*)*E. coli*	FCat fucoidan (*F. vesiculosus*) *S. aureus*
1	n.a.	n.a.	+	+	+	+
2	n.a.	n.a.	+	−	+	−
5	+	+	+	−	−	−
10	+	+	+	−	−	−
50	+	−	+	−	−	−
75	−	−	+	−	n.a.	n.a.
100	−	−	+	−	n.a.	n.a.

[a]"+" indicates the presence of bacteria in the agar plate, whereas "−" indicates the absence of bacteria.

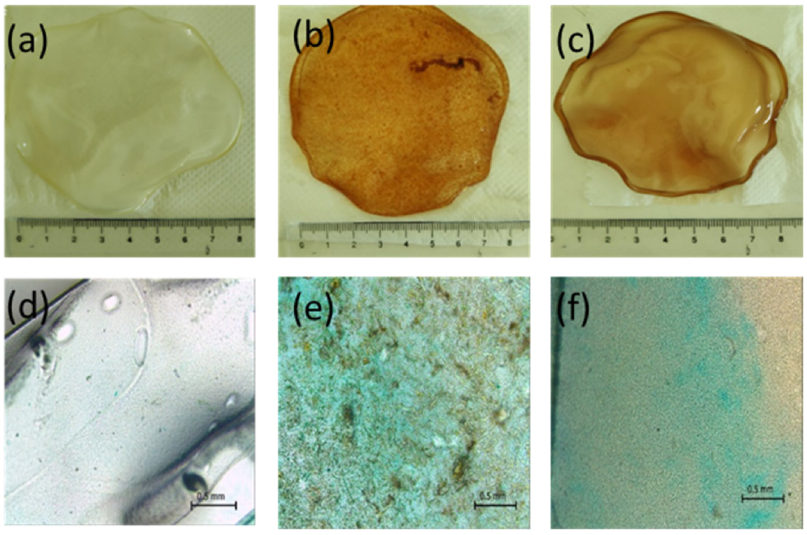

Figure 2. Macroscopic characterization of the developed films. Representative macroscopic images of the films obtained from (a) chitosan (Chit) and blends of chitosan with (b) fucoidan (Chit/F) or (c) modified fucoidan (Chit/FCat). Films were immersed in distilled water prior imaging. Light microscopy images of (d) Chit, (e) Chit/Fuc, and (f) Chit/FCat films stained with Alcian blue. Scale bar is 0.5 mm.

supplemented with Alamar blue (20%) and incubated at 37 °C in a humidified air atmosphere of 5% CO_2 in dark for 4 h. Then, aliquots of 100 μL were transferred to a 96-well black plate and the fluorescence was measured (530 nm excitation wavelength/590 nm emission wavelength) using a microplate reader (BIO-TEK instruments). Cell viability: Live/dead assay (Calcein AM stains the live cells in green and PI stains dead cells in red) was used to assess the viability of L929 cells cultured on the films. After 1, 3, 7, 14, and 21 days, the culture medium was replaced by 500 μL of DMEM supplemented with 1 μg Calcein AM and 0.5 μg PI for 15 min in the dark. The samples were then washed with DPBS and analyzed using an inverted confocal microscope with incubation (TCS SP8, Leica, Germany).

The cytoskeletal organization was visualized by fluorescent microscopy after phalloidin/DAPI staining. At specific time points (1, 3, 7, 14, and 21 days), the medium was removed from the cultures, and the samples were washed with DPBS and fixed with 10% formalin for 30 min. Thereafter, the samples were stained with rhodamine−phalloidin [1:100] for 30 min and with DAPI [1:1000] for 5 min. After washing with DPBS, the samples were analyzed using an inverted confocal microscope with incubation (TCS SP8, Leica, Germany). The number of L929 cells attached to the film was determined by counting cell nuclei stained with DAPI. The nuclei number was assessed with ImageJ (Analysis particles). The results represent the means of three different field-of-view images for each substrate and time point.

2.10. Statistical Analysis. Statistical analysis was performed using OriginPro 2016 software. The results are presented as average ± standard deviation of at least three replicates. Statistical significance was evaluated by one-way analysis of variance (ANOVA) followed by Tukey's test after performing the Shapiro−Wilk test for normal distribution. The p value was set lower than 0.05 and the following symbols were used in the Results and Discussion section: $*p < 0.05$, $**p < 0.01$, $***p < 0.001$.

3. RESULTS AND DISCUSSION

Fucoidan extracted from brown *algae* has various bioactivities, including antibacterial characteristics, that depend on the source and the extraction procedure. Herein, we selected two different *algae* species to obtain fucoidan: *B. bifurcata* due to the abundance on the northeastern Atlantic coast and *F. vesiculosus* because it is one of the most studied fucoidan.[35] *B. bifurcataalgae* were collected, and fucoidan was extracted following a water-based methodology, with yields varying between 1.0 and 2.5%. The FTIR spectrum of fucoidan isolated from *B. bifurcata* was similar to the one of commercial fucoidan (Figure S1 in the Supporting Information). The ^{1}H-NMR spectra were also similar and exhibited the characteristic signals of fucoidans: the signal at 1.23−1.32 ppm corresponding to the H6 methyl protons of L-fucopyranose; the signal of the methyl protons of the *O*-acetyl groups at 2.21 ppm; the signals at 3.43−4.08 ppm corresponding to the ring's protons (H2-H5); the signal at 4.53 ppm associated with the protons of the 4-O-sulfated monosaccharides; and the signals at 5.15 ppm attributed to the C-H proton of substituted O═C and H1 protons of α-L-fucopyranose residues[35−37] (Figures 1b and S2 in the Supporting Information).

The antibacterial potential of the two fucoidans was assessed to establish the amount of fucoidan needed for blending with

https://doi.org/10.1021/acssuschemeng.2c05144
ACS Sustainable Chem. Eng. XXXX, XXX, XXX−XXX

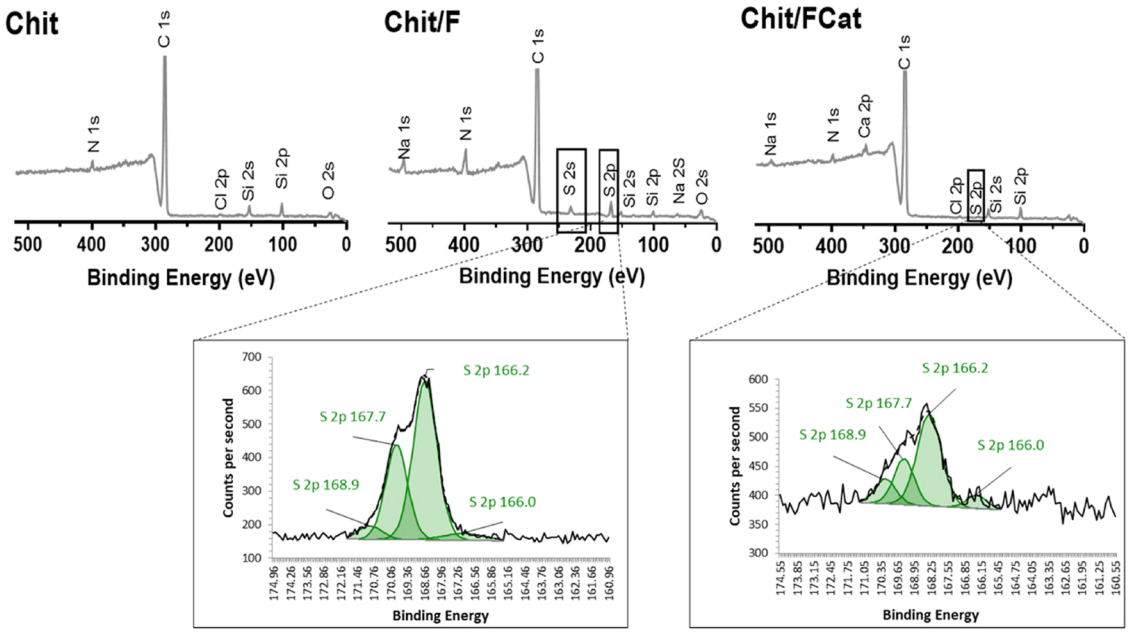

Figure 3. XPS spectra of the studied Chit, Chit/F, and Chit/FCat films and high-resolution sulfur spectra of Chit/F and Chit/FCat films.

Table 2. Surface Wettability (Water Contact Angle) and Surface Energy (SE) Together with Its Components for the Studied Films

sample	Θ water (°)	SE (γ) mN m^{-1}	disp (γ_d) mN m^{-1}	polar (γ_p) mN m^{-1}
Chit	117 ± 3	36.51 ± 0.01	35.50 ± 0.01	1.01 ± 0.00
Chit/F	47 ± 3	51.29 ± 0.09	13.90 ± 0.07	37.39 ± 0.05
Chit/FCat	61 ± 3	43.19 ± 0.05	20.27 ± 0.05	22.92 ± 0.00

chitosan in order to obtain antibacterial films. Fucoidan obtained from *F. vesiculosus* was more efficient in inhibiting the growth of Gram-positive *S. aureus* (MBC of 2 mg/mL) than fucoidan from *B. bifurcata* (MBC of 50 mg/mL). However, fucoidan from *F. vesiculosus* did not reduce the growth of Gram-negative *E. coli*, in contrast to fucoidan from *B. bifurcata* whose MBC was 75 mg/mL (Table 1). Because of the higher efficiency against Gram-positive bacteria, fucoidan from *F. vesiculosus* was functionalized with dopamine to make it more adhesive (Figure 1a). The functionalization was confirmed by ^{1}H-NMR, UV−vis, and FTIR spectroscopies. In the NMR spectrum of FCat, the signal at δ = 6.7−7.5 ppm confirmed the presence of aromatic groups, and the peaks at δ = 3 ppm correspond to the aliphatic protons of dopamine (Figure 1b). The degree of substitution (DS) of FCat was determined from the UV−vis spectrum (Figure 1c). The UV−vis spectrum of FCat showed a characteristic aromatic peak at 280 nm that is not present in the spectrum of native fucoidan. Using this peak and a calibration curve with dopamine solution, we determined a DS of 11%. FTIR spectroscopy supported the modification of FCat through the presence of peaks at 1519 and 1558 cm^{-1}, corresponding to the C═C aromatic stretching and N−H bending (Figure 1d).

Surprisingly, the modification with dopamine groups enhanced the antibacterial properties of fucoidan (Table 1): MBC for FCat was 2 mg/mL for *S. aureus*, i.e. similar to unmodified fucoidan, but the conjugate was also efficient against *E. coli*, with an MBC of 5 mg/mL. Indeed, previous reports describe an antimicrobial activity of catechol derivatives associated with the aromatic portion.[38−41]

Because fucoidan and FCat films were not able to be handled in wet environments, we prepared blended films by adding chitosan to unmodified fucoidan (from *F. vesiculosus*) or its derivative FCat. The obtained films had different macroscopic appearance (Figure 2a−c): pristine chitosan films (Chit) were transparent, the film produced from a combination of fucoidan and chitosan (Chit/F) had a heterogenous orange/brown color, and the films produced from a combination of FCat and chitosan (Chit/FCat) presented a homogenous dark brown color.

Alcian blue staining was performed to detect sulfates in the films. We observed that the control, Chit film, was not stained in blue, confirming the lack of sulfates (Figure 2d). On the other hand, the Chit/F films were blue-stained heterogeneously (Figure 2e), whereas the Chit/FCat films exhibited homogeneous staining with no visible phase separation (Figure 2f). These results indicate that the modification of fucoidan enhances its compatibility with chitosan, most probably via the formation of additional hydrogen bonding, ultimately resulting in a more homogeneous blending of Chit/FCat films.

The incorporation of fucoidan in the films was also confirmed by XPS analysis (Figure 3, Table S2 in the Supporting Information), which showed the emergence of new peaks for S2s and S2p for the fucoidan-containing films. As expected, signals for carbon, oxygen, and nitrogen are present in the spectra of all films because these elements are constituents of chitosan (C, O, N) and fucoidan (C and O) chemical structures. The presence of sodium and chloride is residual and appears due to the use of NaCl to produce the films. In the spectrum of Chit/F films, additional peaks are observed at 174.64−162.60 and 235.71−225.65 eV, which are attributed to sulfur (S2p and S2s, respectively) and associated with the fucoidan presence (Figure

https://doi.org/10.1021/acssuschemeng.2c05144
ACS Sustainable Chem. Eng. XXXX, XXX, XXX−XXX

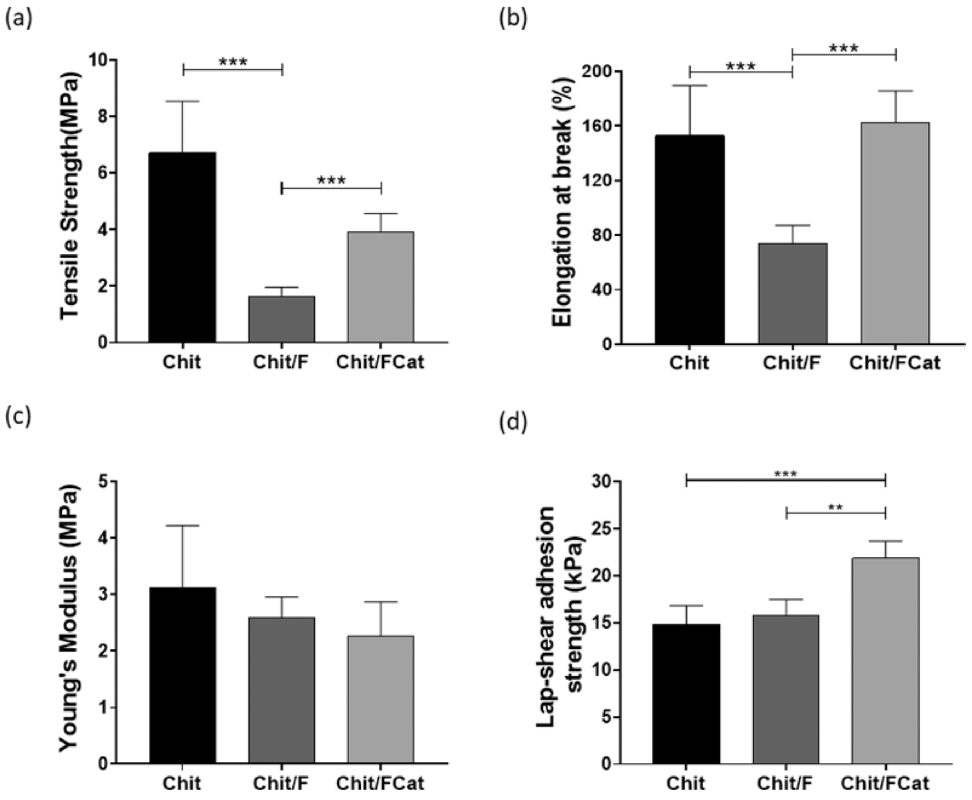

Figure 4. Mechanical properties of the studied films: (a) Tensile strength; (b) elongation at break; (c) Young's modulus; (d) Lap-shear adhesion data for the three studied films. Significant differences are marked with $^{**}p < 0.01$, $^{***}p < 0.001$.

3). The S2p peak was also observed in the spectrum of Chit/FCat (172.12−165.35 eV), while no S signals were detected in the Chit spectrum.

Because material hydrophilicity influences protein adsorption and cell behavior, we also determined the water contact angle and the surface energy (SE) of the films. (Table 2 and Figure S3 in the Supporting Information). Blended films had increased hydrophilicity when compared with the pristine chitosan film. The SE (γ) is a parameter associated not only with the wettability but also with adhesion and friction.[42] The results showed that the addition of fucoidan or its derivative increased the SE of the studied films, with a significant contribution of the polar component. The relation between cell attachment and the SE of films is complex and not always straightforward. The higher SE is associated with high protein adsorption. However, a very high SE can also result in protein denaturation and partial surface passivation that is not favorable for cell attachment. Of note, the used cell culture medium contains a mixture of proteins with different properties and size that compete for the surface (adsorption) area, which makes challenging determination of any specific protein-dependent effects and, consequently, cell behavior.[43−45] These assumptions are also valid in the case of bacterial adhesion.[44,46]

The mechanical properties (tensile strength, elongation at break, and Young's modulus) are essential for a biomaterial/device proper function. Mechanical properties of the films were measured in the wet state and in tensile mode (Figure 4a−c). The tensile strength was higher for Chit (6.72 ± 1.83 MPa) than for Chit/F (1.65 ± 0.31 MPa) and Chit/FCat film (3.92 ± 0.65 MPa). The elongation at break was similar for Chit and Chit/FCat (152.9 ± 36.8 and 162.8 ± 23.0%, respectively) and significantly higher than the one measured for Chit/F films (74.1 ± 13.1%). The high elongation at break is an added value for soft tissue applications as it represents high ductility related to the ability of the films to deform but not break. No significant differences were found in uniaxial elastic Young's modulus (E) of Chit, Chit/F, and Chit/FCat films that were 3.12 ± 1.10, 2.60 ± 0.36, and 2.26 ± 0.61 MPa, respectively, which indicate that the material's stiffness was not altered upon blending. Overall, these data showed that the films have appropriate mechanical properties to be applied in the regeneration of different soft tissues, likely the spinal cord (E = 1.23 MPa),[47] ulnar nerve (E = 5 MPa),[48] or lens capsule (E = 3−4 MPa).[49]

The adhesiveness of the films was assessed in vitro at simulated physiological conditions (Figure 4d). Because an adhesive film prolongs the contact between the material and the wound, it is expected that it will promote an efficient treatment. Chit and Chit/F films detached at a similar strength of about 15 kPa, while a higher strength of 21.89 ± 1.80 kPa was applied to detach the Chit/FCat films. This result is in line with the previous data showing that functionalization with dopamine enhances the adhesion strength of the modified polymers[50−52] Moreover, Scognamiglio et al. reported that the adhesion strength is enhanced during the in vivo applications because of the oxidizing environment of the body that may accelerate the oxidation of hydroxyl groups dopamine, enhancing the bio-adhesion process.[51]

Chit/FCat films showed better adhesion strength than well-known natural tissue adhesives such as chitosan (15 kPa[53]) and fibrin (13.5 kPa[54]) and similar values to synthetic tissue adhesives based on cyanoacrylate (12−40 kPa[55]). Considering the advantages of Chit/FCat films such as sustainable and low-cost raw materials, no risk of disease transmission, we

https://doi.org/10.1021/acssuschemeng.2c05144
ACS Sustainable Chem. Eng. XXXX, XXX, XXX−XXX

hypothesized that the films produced in this study are an excellent alternative to fibrin glue in tissue adhesive applications.

The cytotoxicity of the films was assessed using L929 cultures for up to 21 days as recommended by ISO 10993-5 (Figure 5).

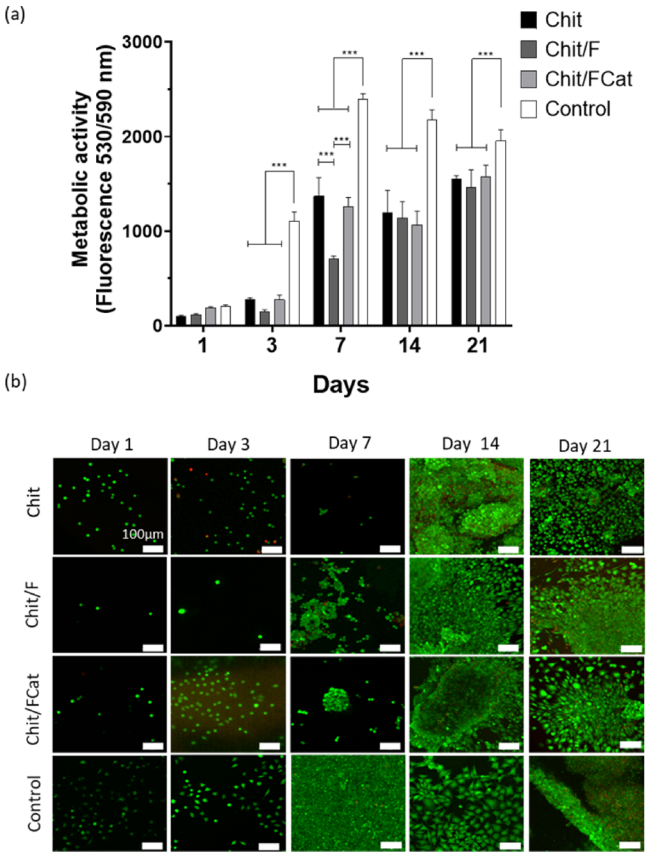

Figure 5. (a) Metabolic activity of L929 cells determined by Alamar blue assay. Significant differences: ***$p < 0.001$. (b) Representative fluorescent images of live (green)/dead (red) cells on the films. Scale bar is 100 μm.

Significant differences in the metabolic activity of cells cultured on the developed films were observed on the first day: L929 cultured on Chit/FCat films presented the highest metabolic activity. However, this difference was not maintained for longer culture times and after 14 days, the cultures on all films had a similar behavior (Figure 5a). The live/dead assay (Figure 5b) showed a minimal number of dead cells (in red), discarding the cytotoxic effect of the films. The number of cells on the films gradually increased with time, reaching the confluence after 14th day of culture and starting to detach from the surface on day 21. On the other hand, the fibroblast culture on TCPS for periods longer than 7 days showed cell overgrowth and detachment. This fibroblasts behavior is evidenced in Figure 5a, which shows that the metabolic activity of fibroblasts on TCPS does not increase from the seventh day onward. It must be pointed out that the films were stable during the 21 days of culture.

The morphology of L929 cells cultured on the films was also evaluated (Figure 6). On the first day of culture, round cells were observed at all conditions. This shape was altered along the culture time: after 7 days, spread spindle-like cells with well-defined actin filaments can be seen on controls (TCPS and Chit) and Chit/FCat films. After 14 days of culture and until the end of the studied period, a cell monolayer that covered the films was

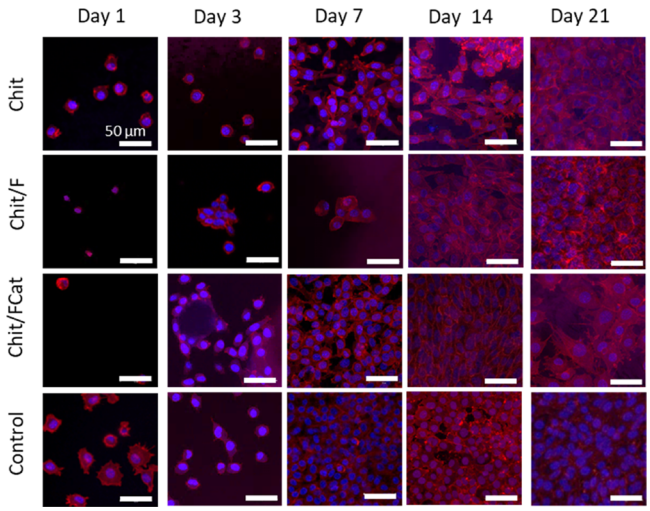

Figure 6. Representative images of L929 cells seeded on the developed films for different culture times and stained for actin (Phalloidin, red) and nuclei (DAPI, blue). Scale bar is 50 μm.

observed and the morphology of the adherent cells on different films was similar.

These results were confirmed by SEM (Figures S4 and S5 in the Supporting Information). SEM images revealed round L929 cells with few filopodia and lamellipodia on Chit films after short culture times (1 and 3 days). At longer culture times (after 7 days and until the end of the experiment), we observed formation of filopodia and lamellipodia and cells elongated to the typical spindle-like morphology.[56] On the other hand, L929 cells seeded on the Chit/FCat films elongated and formed protrusions at an earlier time point, that is, after 3 days of culture. After the 14th day of culture, the cells seeded on the studied films were attached to the surface, with many extending filopodia forming cell clusters on the material. These data agree with previous reports that have shown an important role of catechol groups in promoting cell attachment and proliferation.[57,58]

The number of adherent L929 cells on the studied films and tissue culture polystyrene (TCPS) was evaluated by counting cell nuclei (Fiji ImageJ) after staining with DAPI (Figure 7). The cell density increased with the time of culture, except for the Chit/FCat films, for which the number of cells reached a

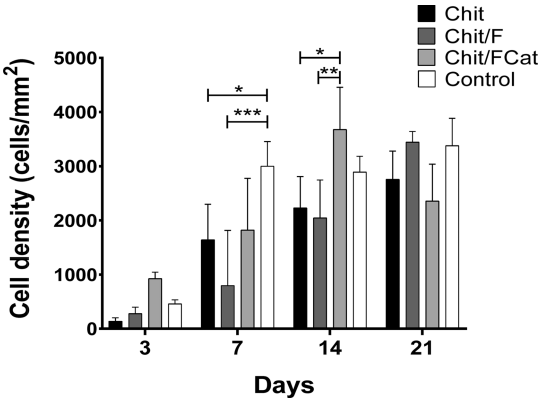

Figure 7. Attachment of L929 cells (number of cells/mm^2) on the studied films (Chit, Chit/F, and Chit/FCat) and control (TCPS) for 3, 7, 14, and 21 days. Significant differences between substrates for the same culture time are marked: *$p < 0.05$, **$p < 0.01$, and **$p < 0.001$.

https://doi.org/10.1021/acssuschemeng.2c05144
ACS Sustainable Chem. Eng. XXXX, XXX, XXX−XXX

maximum on day 14. Longer culture time (21 days) did not result in a further increase of the attached cells on the Chit/FCat because confluence was achieved already at day 14. These results confirmed that catechol functionalization enhanced cell attachment and spreading for shorter periods.

4. CONCLUSIONS

Compared to traditional materials, bioadhesive films are a promising approach for local delivery and/or repair of tissues. Herein, we developed a bioadhesive film using fucoidan derived from *F. vesiculosus*, which was conjugated with dopamine via Schiff base to provide a more adhesive and antibacterial characteristic. The MBC assays showed that the introduction of catechol moieties improved the antibacterial performances of fucoidan, especially in Gram-negative bacteria. The blend of this conjugate with chitosan enhanced adhesive properties to bond the film to the target tissue. Furthermore, the Chit/FCat film supported better fibroblastic cell adhesion, proliferation, and viability than the nonconjugated film.

Overall, considering the advantages of Chit/FCat films, including the low cost, no toxicity, and simplicity, this next-generation adhesive film produced using marine resources might be potentially used as a better alternative for commercial adhesives with antibacterial characteristics for soft tissue repair and/or wound healing.

■ ASSOCIATED CONTENT

Supporting Information

The Supporting Information is available free of charge at https://pubs.acs.org/doi/10.1021/acssuschemeng.2c05144.

Composition of studied films (Table S1); FTIR spectra of fucoidan from *Fucus vesiculosus* and *Bifurcaria bifurcata* (Figure S1); ^{1}H-NMR spectra of fucoidan from *Bifurcaria bifurcata* (Figure S2); elemental quantitative analysis of the surface of films (Table S2); images of water drops placed on films (Figure S3); and SEM images of cells seeded on the Chit and Chit/FCat films (Figures S4 and S5) (PDF)

■ AUTHOR INFORMATION

Corresponding Author

Natália M. Alves − *3B's Research Group, I3Bs − Research Institute on Biomaterials, Biodegradables and Biomimetics, University of Minho, Headquarters of the European Institute of Excellence on Tissue Engineering and Regenerative Medicine, 4805-017 Guimarães, Portugal; ICVS/3B's, Associate PT Government Laboratory, 4710-057 Braga/4805-017 Guimarães, Portugal;* orcid.org/0000-0002-8741-4091; Email: nalves@i3bs.uminho.pt

Authors

Cátia Correia − *3B's Research Group, I3Bs − Research Institute on Biomaterials, Biodegradables and Biomimetics, University of Minho, Headquarters of the European Institute of Excellence on Tissue Engineering and Regenerative Medicine, 4805-017 Guimarães, Portugal; ICVS/3B's, Associate PT Government Laboratory, 4710-057 Braga/4805-017 Guimarães, Portugal*

Diana Soares da Costa − *3B's Research Group, I3Bs − Research Institute on Biomaterials, Biodegradables and Biomimetics, University of Minho, Headquarters of the European Institute of Excellence on Tissue Engineering and Regenerative Medicine, 4805-017 Guimarães, Portugal; ICVS/3B's, Associate PT Government Laboratory, 4710-057 Braga/4805-017 Guimarães, Portugal*

Ana Rita Inácio − *3B's Research Group, I3Bs − Research Institute on Biomaterials, Biodegradables and Biomimetics, University of Minho, Headquarters of the European Institute of Excellence on Tissue Engineering and Regenerative Medicine, 4805-017 Guimarães, Portugal; ICVS/3B's, Associate PT Government Laboratory, 4710-057 Braga/4805-017 Guimarães, Portugal*

A. Catarina Vale − *3B's Research Group, I3Bs − Research Institute on Biomaterials, Biodegradables and Biomimetics, University of Minho, Headquarters of the European Institute of Excellence on Tissue Engineering and Regenerative Medicine, 4805-017 Guimarães, Portugal; ICVS/3B's, Associate PT Government Laboratory, 4710-057 Braga/4805-017 Guimarães, Portugal;* orcid.org/0000-0002-1590-6636

Daniela Peixoto − *3B's Research Group, I3Bs − Research Institute on Biomaterials, Biodegradables and Biomimetics, University of Minho, Headquarters of the European Institute of Excellence on Tissue Engineering and Regenerative Medicine, 4805-017 Guimarães, Portugal; ICVS/3B's, Associate PT Government Laboratory, 4710-057 Braga/4805-017 Guimarães, Portugal*

Tiago H. Silva − *3B's Research Group, I3Bs − Research Institute on Biomaterials, Biodegradables and Biomimetics, University of Minho, Headquarters of the European Institute of Excellence on Tissue Engineering and Regenerative Medicine, 4805-017 Guimarães, Portugal; ICVS/3B's, Associate PT Government Laboratory, 4710-057 Braga/4805-017 Guimarães, Portugal;* orcid.org/0000-0001-8520-603X

Rui L. Reis − *3B's Research Group, I3Bs − Research Institute on Biomaterials, Biodegradables and Biomimetics, University of Minho, Headquarters of the European Institute of Excellence on Tissue Engineering and Regenerative Medicine, 4805-017 Guimarães, Portugal; ICVS/3B's, Associate PT Government Laboratory, 4710-057 Braga/4805-017 Guimarães, Portugal*

Iva Pashkuleva − *3B's Research Group, I3Bs − Research Institute on Biomaterials, Biodegradables and Biomimetics, University of Minho, Headquarters of the European Institute of Excellence on Tissue Engineering and Regenerative Medicine, 4805-017 Guimarães, Portugal; ICVS/3B's, Associate PT Government Laboratory, 4710-057 Braga/4805-017 Guimarães, Portugal;* orcid.org/0000-0001-6818-3374

Complete contact information is available at: https://pubs.acs.org/10.1021/acssuschemeng.2c05144

Author Contributions

The manuscript was written through contributions of all authors. All authors have given approval to the final version of the manuscript.

Notes

The authors declare no competing financial interest.

■ ACKNOWLEDGMENTS

The authors acknowledge the Portuguese Foundation for Science and Technology (FCT) and the European program FEDER/FEEI for the financial support through the PTDC/BTM-MAT/28123/2017 project. FCT is also acknowledged for the PhD scholarship SFRH/BD/143209/2019 granted to C.C. This article has also been prepared with the support of REMIX Project, funded by the European Union's Horizon 2020 Research and Innovation programme under the Maria

Sklodowska-Curie grant agreement no. 778078. Dr. Luisa Rodrigues is acknowledged for performing the XPS analysis.

REFERENCES

(1) Ahmed, W.; Zhai, Z.; Gao, C. Adaptive antibacterial biomaterial surfaces and their applications. *Mater. Today Bio* **2019**, *2*, No. 100017.
(2) Campoccia, D.; Montanaro, L.; Arciola, C. R. A review of the clinical implications of anti-infective biomaterials and infection-resistant surfaces. *Biomaterials* **2013**, *34*, 8018−8029.
(3) Shannon, E.; Abu-Ghannam, N. Antibacterial Derivatives of Marine Algae: An Overview of Pharmacological Mechanisms and Applications. *Mar. Drugs* **2016**, *14*, 81.
(4) Fitton, H. J.; Stringer, D. S.; Park, A. Y.; Karpiniec, S. N. Therapies from Fucoidan: New Developments. *Mar. Drugs* **2019**, *17*, 571.
(5) Wang, Y.; Wang, Q.; Han, X.; Ma, Y.; Zhang, Z.; Zhao, L.; Guan, F.; Ma, S. Fucoidan: a promising agent for brain injury and neurodegenerative disease intervention. *Food Funct.* **2021**, *12*, 3820−3830.
(6) Jin, J. O.; Chauhan, P. S.; Arukha, A. P.; Chavda, V.; Dubey, A.; Yadav, D. The Therapeutic Potential of the Anticancer Activity of Fucoidan: Current Advances and Hurdles. *Mar. Drugs* **2021**, *19*, 265.
(7) Wang, J.; Zhang, Q.; Zhang, Z.; Hou, Y.; Zhang, H. In-vitro anticoagulant activity of fucoidan derivatives from brown seaweed Laminaria japonica. *Chinese J. Oceanol. Limnol.* **2011**, *29*, 679−685.
(8) Wang, L.; Jayawardena, T. U.; Yang, H. W.; Lee, H. G.; Kang, M. C.; Sanjeewa, K. K. A.; Oh, J. Y.; Jeon, Y. J. Isolation, Characterization, and Antioxidant Activity Evaluation of a Fucoidan from an Enzymatic Digest of the Edible Seaweed, Hizikia fusiforme. *Antioxidants* **2020**, *9*, 363.
(9) Reys, L. L.; Silva, S. S.; Oliveira, C.; Neves, N. M.; Martins, A.; Reis, R. L.; Silva, T. H. Angiogenic potential of airbrushed fucoidan/polycaprolactone nanofibrous meshes. *Int. J. Biol. Macromol.* **2021**, *183*, 695−706.
(10) Oliveira, C.; Granja, S.; Neves, N. M.; Reis, R. L.; Baltazar, F.; Silva, T. H.; Martins, A. Fucoidan from Fucus vesiculosus inhibits new blood vessel formation and breast tumor growth in vivo. *Carbohydr. Polym.* **2019**, *223*, No. 115034.
(11) Oliveira, C.; Soares, A. I.; Neves, N. M.; Reis, R. L.; Marques, A. P.; Silva, T. H.; Martins, A. Fucoidan Immobilized at the Surface of a Fibrous Mesh Presents Toxic Effects over Melanoma Cells, But Not over Noncancer Skin Cells. *Biomacromolecules* **2020**, *21*, 2745−2754.
(12) Wu, S. Y.; Wu, A. T.; Yuan, K. S.; Liu, S. H. Brown Seaweed Fucoidan Inhibits Cancer Progression by Dual Regulation of mir-29c/ADAM12 and miR-17-5p/PTEN Axes in Human Breast Cancer Cells. *J. Cancer* **2016**, *7*, 2408−2419.
(13) Wang, W.; Wu, J.; Zhang, X.; Hao, C.; Zhao, X.; Jiao, G.; Shan, X.; Tai, W.; Yu, G. Inhibition of Influenza A Virus Infection by Fucoidan Targeting Viral Neuraminidase and Cellular EGFR Pathway. *Sci. Rep.* **2017**, *7*, 40760.
(14) Ahmadi, A.; Zorofchian Moghadamtousi, S.; Abubakar, S.; Zandi, K. Antiviral Potential of Algae Polysaccharides Isolated from Marine Sources: A Review. *Biomed. Res. Int.* **2015**, *2015*, No. 825203.
(15) Thuy, T. T.; Ly, B. M.; Van, T. T.; Quang, N. V.; Tu, H. C.; Zheng, Y.; Seguin-Devaux, C.; Mi, B.; Ai, U. Anti-HIV activity of fucoidans from three brown seaweed species. *Carbohydr. Polym.* **2015**, *115*, 122−128.
(16) Takahashi, H.; Kawaguchi, M.; Kitamura, K.; Narumiya, S.; Kawamura, M.; Tengan, I.; Nishimoto, S.; Hanamure, Y.; Majima, Y.; Tsubura, S.; Teruya, K.; Shirahata, S. An Exploratory Study on the Anti-inflammatory Effects of Fucoidan in Relation to Quality of Life in Advanced Cancer Patients. *Integr. Cancer Ther.* **2018**, *17*, 282−291.
(17) Xu, Y.; Xu, J.; Ge, K.; Tian, Q.; Zhao, P.; Guo, Y. Anti-inflammatory effect of low molecular weight fucoidan from Saccharina japonica on atherosclerosis in apoE-knockout mice. *Int. J. Biol. Macromol.* **2018**, *118*, 365−374.
(18) Palanisamy, S.; Vinosha, M.; Rajasekar, P.; Anjali, R.; Sathiyaraj, G.; Marudhupandi, T.; Selvam, S.; Prabhu, N. M.; You, S. Antibacterial efficacy of a fucoidan fraction (Fu-F2) extracted from Sargassum polycystum. *Int. J. Biol. Macromol.* **2019**, *125*, 485−495.
(19) Ayrapetyan, O. N.; Obluchinskaya, E. D.; Zhurishkina, E. V.; Skorik, Y. A.; Lebedev, D. V.; Kulminskaya, A. A.; Lapina, I. M. Antibacterial Properties of Fucoidans from the Brown Algae Fucus vesiculosus L. of the Barents Sea. *Biology* **2021**, *10*, 67.
(20) Perumal, R. K.; Perumal, S.; Thangam, R.; Gopinath, A.; Ramadass, S. K.; Madhan, B.; Sivasubramanian, S. Collagen-fucoidan blend film with the potential to induce fibroblast proliferation for regenerative applications. *Int. J. Biol. Macromol.* **2018**, *106*, 1032−1040.
(21) Benbow, N. L.; Karpiniec, S.; Krasowska, M.; Beattie, D. A. Incorporation of FGF-2 into Pharmaceutical Grade Fucoidan/Chitosan Polyelectrolyte Multilayers. *Mar. Drugs* **2020**, *18*, 531.
(22) Sun, F.; Bu, Y.; Chen, Y.; Yang, F.; Yu, J.; Wu, D. An Injectable and Instant Self-Healing Medical Adhesive for Wound Sealing. *ACS Appl. Mater. Interfaces* **2020**, *12*, 9132−9140.
(23) Pandey, N.; Soto-Garcia, L. F.; Liao, J.; Philippe, Z.; Nguyen, K. T.; Hong, Y. Mussel-inspired bioadhesives in healthcare: design parameters, current trends, and future perspectives. *Biomater. Sci.* **2020**, *8*, 1240−1255.
(24) Zhang, C.; Wu, B.; Zhou, Y.; Zhou, F.; Liu, W.; Wang, Z. Mussel-inspired hydrogels: from design principles to promising applications. *Chem. Soc. Rev.* **2020**, *49*, 3605−3637.
(25) Lee, S. Y.; Lee, J. N.; Chathuranga, K.; Lee, J. S.; Park, W. H. Tunicate-inspired polyallylamine-based hydrogels for wet adhesion: A comparative study of catechol- and gallol-functionalities. *J. Colloid Interface Sci.* **2021**, *601*, 143−155.
(26) Jeong, Y.; Thuy, L. T.; Ki, S. H.; Ko, S.; Kim, S.; Cho, W. K.; Choi, J. S.; Kang, S. M. Multipurpose Antifouling Coating of Solid Surfaces with the Marine-Derived Polymer Fucoidan. *Macromol. Biosci.* **2018**, *18*, No. e1800137.
(27) Kim, C. H.; Park, S. J.; Yang, D. H.; Chun, H. J. Chitosan for Tissue Engineering. *Adv. Exp. Med. Biol.* **2018**, *1077*, 475−485.
(28) Rodriguez-Vazquez, M.; Vega-Ruiz, B.; Ramos-Zuniga, R.; Saldana-Koppel, D. A.; Quinones-Olvera, L. F. Chitosan and Its Potential Use as a Scaffold for Tissue Engineering in Regenerative Medicine. *Biomed. Res. Int.* **2015**, *2015*, No. 821279.
(29) Barbosa, A. I.; Costa Lima, S. A.; Reis, S. Development of methotrexate loaded fucoidan/chitosan nanoparticles with anti-inflammatory potential and enhanced skin permeation. *Int. J. Biol. Macromol.* **2019**, *124*, 1115−1122.
(30) Sezer, A. D.; Cevher, E.; Hatipoglu, F.; Ogurtan, Z.; Bas, A. L.; Akbuga, J. Preparation of Fucoidan-Chitosan Hydrogel and Its Application as Burn Healing Accelerator on Rabbits. *Biol. Pharm. Bull.* **2008**, *31*, 2326−2333.
(31) Hao, Y.; Zhao, W.; Zhang, L.; Zeng, X.; Sun, Z.; Zhang, D.; Shen, P.; Li, Z.; Han, Y.; Li, P.; Zhou, Q. Bio-multifunctional alginate/chitosan/fucoidan sponges with enhanced angiogenesis and hair follicle regeneration for promoting full-thickness wound healing. *Mater. Des.* **2020**, *193*, No. 108863.
(32) Signini, R.; Campana, S. P. Características e Propriedades de Quitosanas Purificadas nas Formas Neutra, Acetato e Cloridrato. *Polímeros* **2001**, *11*, 58−64.
(33) Yang, C.; Chung, D.; Shin, I. S.; Lee, H.; Kim, J.; Lee, Y.; You, S. Effects of molecular weight and hydrolysis conditions on anticancer activity of fucoidans from sporophyll of Undaria pinnatifida. *Int. J. Biol. Macromol.* **2008**, *43*, 433−437.
(34) Castle, J. E. Practical surface analysis by Auger and X-ray photoelectron spectroscopy. *Surf. Interface Anal.* **1984**, *6*, 302.
(35) Bittkau, K. S.; Dorschmann, P.; Blumel, M.; Tasdemir, D.; Roider, J.; Klettner, A.; Alban, S. Comparison of the Effects of Fucoidans on the Cell Viability of Tumor and Non-Tumor Cell Lines. *Mar. Drugs* **2019**, *17*, 441.
(36) Kariya, Y.; Mulloy, B.; Imai, K.; Tominaga, A.; Kaneko, T.; Asari, A.; Suzuki, K.; Masuda, H.; Kyogashima, M.; Ishii, T. Isolation and partial characterization of fucan sulfates from the body wall of sea cucumber Stichopus japonicus and their ability to inhibit osteoclastogenesis. *Carbohydr. Res.* **2004**, *339*, 1339−1346.
(37) Bouissil, S.; Alaoui-Talibi, Z. E.; Pierre, G.; Rchid, H.; Michaud, P.; Delattre, C.; El Modafar, C. Fucoidans of Moroccan Brown Seaweed

https://doi.org/10.1021/acssuschemeng.2c05144
ACS Sustainable Chem. Eng. XXXX, XXX, XXX−XXX

as Elicitors of Natural Defenses in Date Palm Roots. *Mar. Drugs* **2020**, *18*, 596.
(38) Razaviamri, S.; Wang, K.; Liu, B.; Lee, B. P. Catechol-Based Antimicrobial Polymers. *Molecules* **2021**, *26*, 559.
(39) Daglia, M. Polyphenols as antimicrobial agents. *Curr. Opin. Biotechnol.* **2012**, *23*, 174−181.
(40) Bostan, H.; Tomak, Y.; Karaoglu, S. A.; Erdivanli, B.; Hanci, V. In vitro evaluation of antimicrobial features of vasopressors. *Braz. J. Anesthesiol.* **2014**, *64*, 84−88.
(41) Liu, B.; Zhou, C.; Zhang, Z.; Roland, J. D.; Lee, B. P. Antimicrobial Property of Halogenated Catechols. *Chem. Eng. J.* **2021**, *403*, No. 126340.
(42) Kozbial, A.; Li, Z.; Conaway, C.; McGinley, R.; Dhingra, S.; Vahdat, V.; Zhou, F.; D'Urso, B.; Liu, H.; Li, L. Study on the surface energy of graphene by contact angle measurements. *Langmuir* **2014**, *30*, 8598−8606.
(43) Norde, W.; Lyklema, J. Why proteins prefer interfaces. *J. Biomater. Sci. Polym. Ed.* **1991**, *2*, 183−202.
(44) Busscher, H. J.; Weerkamp, A. H.; Van der Mei, H. C.; Van Pelt, A. W. J.; De Jong, H. P.; Arends, J. Measurement of the Surface Free Energy of Bacterial Cell Surfaces and Its Relevance for Adhesion. *Appl. Environ. Microbiol.* **1984**, *48*, 980−983.
(45) Comelles, J.; Estevez, M.; Martinez, E.; Samitier, J. The role of surface energy of technical polymers in serum protein adsorption and MG-63 cells adhesion. *Nanomedicine* **2010**, *6*, 44−51.
(46) Lorenzetti, M.; Dogsa, I.; Stosicki, T.; Stopar, D.; Kalin, M.; Kobe, S.; Novak, S. The influence of surface modification on bacterial adhesion to titanium-based substrates. *ACS Appl. Mater. Interfaces* **2015**, *7*, 1644−1651.
(47) Oakland, R. J.; Hall, R. M.; Wilcox, R. K.; Barton, D. C. The biomechanical response of spinal cord tissue to uniaxial loading. *Proc. Inst. Mech. Eng. H* **2006**, *220*, 489−492.
(48) Ma, Z.; Hu, S.; Tan, J. S.; Myer, C.; Njus, N. M.; Xia, Z. In vitro and in vivo mechanical properties of human ulnar and median nerves. *J. Biomed. Mater. Res. A* **2013**, *101*, 2718−2725.
(49) Krag, S.; Andreassen, T. T. Mechanical properties of the human lens capsule. *Prog. Retin. Eye Res.* **2003**, *22*, 749−767.
(50) Gowda, A. H. J.; Bu, Y.; Kudina, O.; Krishna, K. V.; Bohara, R. A.; Eglin, D.; Pandit, A. Design of tunable gelatin-dopamine based bioadhesives. *Int. J. Biol. Macromol.* **2020**, *164*, 1384−1391.
(51) Scognamiglio, F.; Travan, A.; Borgogna, M.; Donati, I.; Marsich, E.; Bosmans, J. W.; Perge, L.; Foulc, M. P.; Bouvy, N. D.; Paoletti, S. Enhanced bioadhesivity of dopamine-functionalized polysaccharidic membranes for general surgery applications. *Acta Biomater.* **2016**, *44*, 232−242.
(52) Sousa, M. P.; Neto, A. I.; Correia, T. R.; Miguel, S. P.; Matsusaki, M.; Correia, I. J.; Mano, J. F. Bioinspired multilayer membranes as potential adhesive patches for skin wound healing. *Biomater. Sci.* **2018**, *6*, 1962−1975.
(53) Lauto, A.; Mawad, D.; Foster, L. J. R. Adhesive biomaterials for tissue reconstruction. *J. Chem. Technol. Biotechnol.* **2008**, *83*, 464−472.
(54) Bhagat, V.; Becker, M. L. Degradable Adhesives for Surgery and Tissue Engineering. *Biomacromolecules* **2017**, *18*, 3009−3039.
(55) Singer, A. J.; Perry, L. A comparative study of the surgically relevant mechanical characteristics of the topical skin adhesives. *Acad. Emerg. Med.* **2012**, *19*, 1281−1286.
(56) Zhang, W. C.; Zheng, M. L.; Liu, J.; Jin, F.; Dong, X. Z.; Guo, M.; Li, T. Modulation of Cell Behavior by 3D Biocompatible Hydrogel Microscaffolds with Precise Configuration. *Nanomaterials* **2021**, *11*, 2325.
(57) Suneetha, M.; Rao, K. M.; Han, S. S. Mussel-Inspired Cell/Tissue-Adhesive, Hemostatic Hydrogels for Tissue Engineering Applications. *ACS Omega* **2019**, *4*, 12647−12656.
(58) Zhou, D.; Li, S.; Pei, M.; Yang, H.; Gu, S.; Tao, Y.; Ye, D.; Zhou, Y.; Xu, W.; Xiao, P. Dopamine-Modified Hyaluronic Acid Hydrogel Adhesives with Fast-Forming and High Tissue Adhesion. *ACS Appl. Mater. Interfaces* **2020**, *12*, 18225−18234.

https://doi.org/10.1021/acssuschemeng.2c05144
ACS Sustainable Chem. Eng. XXXX, XXX, XXX−XXX